

Biomechanics of budding of cellular membranes

Aleš Iglič, Maruša Lokar, Peter Veranič, Henry Hägerstrand, Veronika Kralj-Iglič

Abstract—Biomechanics of the cell shape changes and the budding of the cellular membrane is described. It is indicated that two mechanisms based on internal degrees of freedom: in-plane orientational ordering of membrane constituents and non-homogeneous lateral distribution of membrane constituents, are complementary mechanisms that may promote budding of the membrane and determine the shape of the released daughter vesicle (spherical or tubular). Tubular budding may be explained by self-assembly of anisotropic membrane nanodomains into larger domains forming nanotubular membrane protrusions. In contrast to some previously reported theories, no direct external mechanical force is needed to explain the tubular budding of cellular membrane. The mechanism that explains tubular budding may also be responsible for stabilization of tunneling nanotubes (TNT) that connect cells and are important for transport of matter and information in cellular systems.

Index Terms—cell biomechanics; anisotropy; membrane free energy; tunneling nanotubes

I. INTRODUCTION

EXOGENOUSLY added amphiphilic substances (detergents, peptides) bind readily into the red blood cell membrane, thereby causing cell shape changes. According to the bilayer couple hypothesis, the transformation of echinocyte shape is driven by binding of the exogenously added molecules preferentially into the outer membrane layer (Fig.1). When red blood cells approach to the type III echinocytic shape, budding and nanoexovesicle release (spherical or tubular) from the membrane surface starts (Fig.1)

II. THEORY

It has been shown that the stability of the echinocyte shape is primarily determined by competition between the membrane bilayer Helfrich-Evans bending energy and the membrane skeleton shear energy (Fig. 2) For reasons of simplicity the membrane skeleton shear energy is usually calculated using an approximate expression [3], [1]:

$$W_{\text{shear}} = \frac{\mu}{2} \int (\lambda_m^2 + \lambda_m^{-2} - 2) dA, \quad (1)$$

where the membrane skeleton is considered laterally incompressible, μ is the membrane skeleton area shear modulus, λ_m is the principal extension ratio along the meridional direction [3], [1] and dA is the membrane area

A. Iglič and M. Lokar are with the Laboratory of Physics, Faculty of Electrical Engineering, University of Ljubljana, Ljubljana, Slovenia. P. Veranič is with the Institute of Cell Biology, Faculty of Medicine, University of Ljubljana, Ljubljana, Slovenia. H. Hägerstrand is with the Department of Biology, Åbo Akademi University, Biocity, Åbo/Turku, Finland. V. Kralj-Iglič is with the Laboratory of Clinical Biophysics, Faculty of Medicine, University of Ljubljana, Ljubljana, Slovenia. email: ales.iglic@fe.uni-lj.si; phone: + 386 1 4768 825; fax: +386 1 4768 850

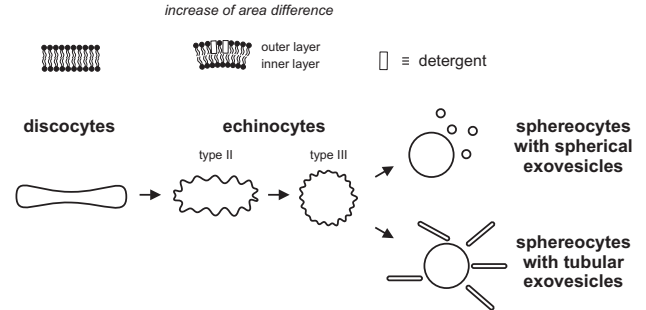


Fig. 1. Schematic figure of erythrocyte shape transformations due to preferential intercalation of a detergent into the outer membrane layer. At low detergent concentrations echinocytes of type I and II appear in the erythrocyte suspension, while at higher molecular concentrations echinocytes of type III are the most frequent. At still higher molecular concentrations, i.e. at sublytic molecular concentrations the budding (exovesiculation) and release of spherical or tubular vesicles start (see also [2] and references therein). As a result the erythrocytes are transformed into sphereocytes.

element. The Helfrich-Evans membrane bending energy is the sum of a local and a non-local term [3], [4]:

$$W_b = \frac{k_c}{2} \int (2H)^2 dA + k_n A (\langle H \rangle - H_0)^2, \quad (2)$$

where $H = (C_1 + C_2)/2$ is the local mean curvature of the membrane, C_1 and C_2 are the two principal curvatures describing the local shape of the membrane surface, $\langle H \rangle = \int H dA/A$ is the average mean curvature, H_0 is the effective spontaneous mean curvature [3], k_c is the membrane isotropic bending constant, k_n is the coefficient of nonlocal bending rigidity [3] and A is the membrane area. For thin and not too strongly curved bilayers the average mean curvature $\langle H \rangle$ is proportional to the difference between the two membrane monolayer areas (ΔA): $\langle H \rangle = \Delta A/2A\delta$, where δ is the distance between the two monolayer neutral surfaces. The normalized average mean curvature $\langle h \rangle = R_0 \langle H \rangle$ is equal to the normalized area difference $\Delta a = \Delta A/8\pi\delta R_0$, where R_0 is defined as $R_0 = \sqrt{A/4\pi}$. The normalized effective spontaneous mean curvature $h_0 = R_0 H_0$ is equal to the normalized optimal area difference Δa_0 : $h_0 = \Delta a_0 = \Delta A_0/8\pi\delta R_0$.

The spherical erythrocyte shape (sphereocyte) at sublytic concentrations of echinocytogenic detergents arises due to reducing the size of echinocyte spicules. The spicules become smaller mainly due to release of daughter exovesicles from the cell surface (Fig.1), predominantly from the echinocyte spicules. Most of the hitherto studied echinocytogenic detergents induce spherical budding and nanoexovesicles, while strongly anisotropic detergent molecules (for example dimeric detergents or detergents with a dimeric headgroup [2]) were found to induce

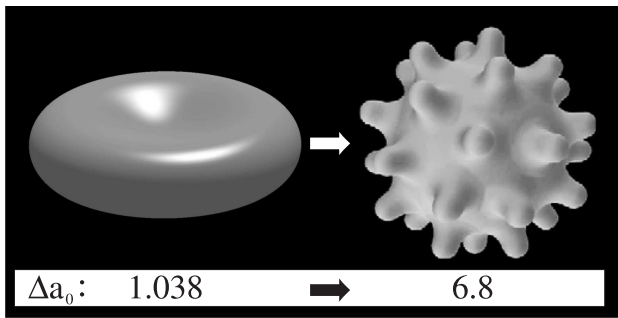


Fig. 2. The calculated erythrocyte shapes determined by minimization of the membrane elastic energy (bending and shear) for two different values of Δa_0 [1], [4].

mainly tubular buds and tubular nanoexovesicles. The tubular budding observed does not need any additional driving (pulling) force. Since the spherical and tubular daughter nanovesicles released from the erythrocyte membrane are highly depleted in the membrane skeleton, the shape of buds/vesicles is determined by the properties of the membrane bilayer. It is of interest to understand the mechanisms which determine the observed detergent-induced tubular budding of the bilayer membrane. It is generally accepted that the standard theory of isotropic membrane elasticity which is based on a description of the membrane as a bilayer composed of two compressible isotropic monolayers does not provide an explanation for tubular budding (as observed in this work) if no pulling force is applied. In this work we explain the observed tubular budding of the cell membrane by accumulation of anisotropic membrane constituents in the tubular budding region [2], [4]. Without the anisotropic membrane constituents, spherical budding is always energetically favourable.

Much experimental and theoretical evidence indicates the existence of membrane micro and nanodomains. In the model we assume that membrane nanodomains (Fig.3), as a result of their structure and local interactions energetically prefer a local geometry that is described by the two intrinsic principal curvatures (C_{1m} and C_{2m}). The intrinsic principal curvatures (spontaneous curvatures) (C_{1m} and C_{2m}) are in general different ($C_{1m} \neq C_{2m}$) (Fig. 3). If they are identical ($C_{1m} = C_{2m}$), the nanodomain is called isotropic. If $C_{1m} \neq C_{2m}$ the nanodomain is called anisotropic. The orientation of the anisotropic nanodomain is important for its energy. An anisotropic nanodomain will on the average spend more time in the orientation that is energetically more favourable than in any other orientation.

The elastic energy of the membrane nanodomain per unit area (w) should be a scalar quantity. Therefore each term in the expansion of w must also be scalar [6], *i.e.* invariant with respect to all transformations of the local coordinate system. In this work, the elastic energy of the single membrane (in general isotropic) nanodomain is expressed

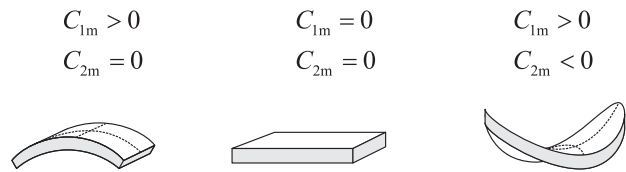


Fig. 3. Schematic representation of three different intrinsic shapes of membrane flexible nanodomains (cylindrical, flat and saddle-like shapes). Different intrinsic shapes are described by the two intrinsic principal curvatures C_{1m} and C_{2m} [2], [4].

as [2], [4], [6]:

$$f_i = (2K_1 + K_2)(H - H_m)^2 a_0 + K_2(D^2 + D_m^2)a_0 - kT \ln \left(I_0 \left(\frac{2K_2 D D_m a_0}{kT} \right) \right) \quad (3)$$

where k is Boltzmann constant, T absolute temperature, I_0 is modified Bessel function, $(C_1 - C_2)/2$ is the membrane curvature deviator, $H_m = (C_{1m} + C_{2m})/2$ is the intrinsic (spontaneous) mean curvature and $D_m = (C_{1m} - C_{2m})/2$ is the intrinsic (spontaneous) curvature deviator, a_0 is the area of single nanodomain, while K_1 and K_2 are elastic constants. It can be seen from Eq.(3) that the material properties of an anisotropic flexible membrane nanodomain can be expressed in a simple way by only two intrinsic curvatures C_{1m} and C_{2m} . The free energy of bilayer cell membrane containing flexible nanodomains can be therefore expressed as (see also [2], [4], [6]):

$$F/(A/a_0) = kT \int n \ln n \, da + kT \int (1 - n) \ln(1 - n) \, da + \frac{k_c a_0}{2} \int (2H)^2 (1 - n) \, da + 2w \int n^2 da + \int n f_i \, da \quad (4)$$

where n is the fraction of the membrane area covered by nanodomains, w is the nearest-neighbor energy between the inclusions, Integration goes over the entire (normalized) area of the membrane surface ($\int da = 1$). The first two terms in Eq.(4) represent the configurational entropy, the third term represents the local bending energy, the fourth term represents the energy of nearest-neighbour interactions between the inclusions and the fifth term represents the energy of inclusions. The membrane free energy is minimized to yield the equilibrium shape of the membrane and the lateral and orientational distribution functions of membrane constituents (nanodomains) in the budding region.

We showed that membrane skeleton-detached, laterally mobile membrane nanodomains (inclusions) may sort into curved membrane budding regions, depending on their intrinsic molecular shape and/or direct interactions between the raft elements [5]. Also it was shown that tubular budding of cellular membrane may be explained

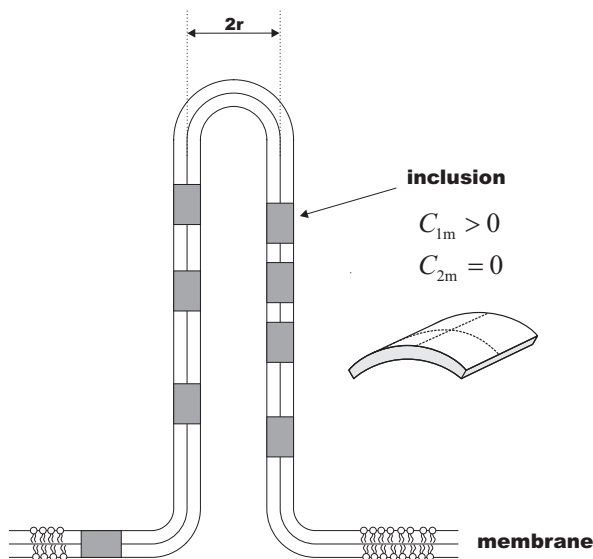


Fig. 4. Schematic illustration of stabilisation of nanotubular membrane protrusions by accumulation of anisotropic membrane nanodomains (inclusions) in the region of the nanotube. Possible candidates for anisotropic membrane nanodomains (inclusions) might be prominin-containing nanodomains [7], [8]. The cylindrical shaped anisotropic membrane domains, once assembled in the membrane region of a nanotubular membrane protrusion, are keeping the protrusion mechanically stable even if the cytoskeletal components (actin filaments) are not present in the nanotube [4], [10].

by self-assembly of anisotropic membrane nanodomains (inclusions) into larger domains forming the nanotubular membrane protrusions (Fig.4) [4], [2].

III. TUNNELING NANOTUBES

The mechanism similar to that as proposed to explain the growth and stability of tubular protrusions of cellular (erythrocyte) membranes may also be responsible for the stability of observed tunneling nanotubes connecting two cellular compartments (Fig.5) which may be important in the transport of matter and information in cellular systems [9], [4], [10].

In our model we assume that anisotropic membrane nanodomains (inclusions) (Fig.4) 12), as a result of their structure and local interactions energetically prefer to accumulate in the membrane region of tunneling nanotubes with the principal curvatures C_1 and C_2 close to the values of its intrinsic principal curvatures C_{1m} and C_{2m} [4], [10]. The curvature mediated accumulation of interacting anisotropic membrane nanodomains (inclusions) having $C_{1m} > 0$ and $C_{2m} \approx 0$, which prefer cylindrical shape of the membrane (see Figs.12,13), in tunneling nanotubes might thus create a phase separation with respect to the surrounding microenvironment [4], [10]. The self-assembly of interacting nanodomains which prefer cylindrical membrane shape into larger tubular domains may thus explain the stability of tunneling nanotubes even if there are no actin fibers generating a pulling or pushing force (Fig.4) [4], [10].

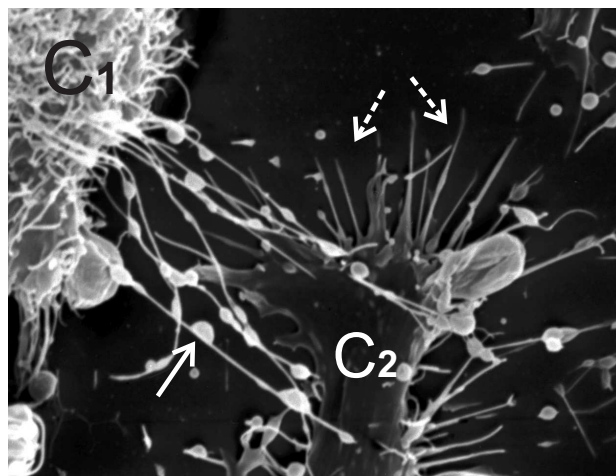


Fig. 5. A scanning electron micrograph of two T24 cells connected by nanotubes with dilations, which are integral part of the nanotubes (white arrow). Membrane of one cell (C1) has many small membrane protrusions, while membrane of second cell (C2) is rather smooth with many filopodia searching the surroundings (dashed arrow).

IV. CONCLUSIONS

We described the sorting of flexible membrane nanodomains (inclusions) in the process of membrane budding. In contrast to some previously reported theories, no direct external mechanical force is needed to explain the observed tubular budding of the bilayer membrane. The mechanism that explains tubular budding may also be responsible for stabilization of the thin tubes that connect cells or cell organelles (tunneling nanotubes) and which might be important for transport of matter and information in cellular systems.

REFERENCES

- [1] Igljč, A., A possible mechanism determining the stability of spiculated red blood cells, *J. Biomech.*, **30**, 1997, 35–40.
- [2] Kralj-Igljč, V., Hägerstrand, H., Veranič, V., Jezernik, K. and Igljč, A., Amphiphile-induced tubular budding of the bilayer membrane, *Eur. Biophys. J.*, **34**, 2005, 1066–1070.
- [3] Evans, E.A. and R. Skalak, *Mechanics and thermodynamics of biomembranes*, CRC Press, Boca Raton, 1980.
- [4] Igljč, A., Lokar, M., Babnik, B., Slivnik, T., Veranič, P., Hägerstrand, H. and Kralj-Igljč, V., Possible role of flexible red blood cell membrane nanodomains in the growth and stability of membrane nanotubes, *Blood Cells Mol. Dis.*, **39**, 2007, 14–23.
- [5] Igljč, A., Babnik, B., Fošnarič, M., Hägerstrand, H. and Kralj-Igljč, V., On the role of anisotropy of membrane constituents in formation of a membrane neck during budding of multicomponent membrane, *J. Biomech.*, **40**, 2007, 579–585.
- [6] Igljč, A., Slivnik, T. and Kralj-Igljč, V., Elastic properties of biological membranes influenced by attached proteins, *J. Biomech.*, **40**, 2007, 2492–2500.
- [7] Igljč, A., H. Hägerstrand, P. Veranič, A. Plemenitaš, and V. Kralj-Igljč, Curvature induced accumulation of anisotropic membrane components and raft formation in cylindrical membrane protrusions, *J. Theor. Biol.*, **240**, 2006, 368–373.
- [8] Janich, P., and D. Corbeil, GM1 and GM3 gangliosides highlight distinct lipid microdomains with the apical domain of epithelial cells, *FEBS Lett.*, **581**, 2007, 1783–1787.
- [9] Rustom, A., Saffrich, R., Marković, I., Walther, P. and Gerdes, H.H., Nanotubular highways for intercellular organelle transport, *Science*, **303**, 2004, 1007–1010.

- [10] Veranič, P., Lokar, M., Schuetz, G.J., Weghuber, J., Wieser, S., Hägerstrand, H., Kralj-Iglič, V. and Iglič A.: Different types of cell-to-cell connections mediated by nanotubular structures, *Biophys. J.* , **25**, 2008 (in print).